Management of flood and separating damage from environmental effects using Bayesian convolutional neural network

Muthulakshmi K.[1,*], Mohan V.[2], Sundar Prakash Balaji.[3] and Revathi K.[4]
[1]ECE, Sri Krishna College of Technology, Coimbatore, Tamil Nadu, India
[2]Department of ECE, Saranathan College of Engineering, Panjapur, Trichy-620012, Tamil Nadu, India
[3]ECE, Mookambigai College of Engineering, Keeranur, Pudukkottai, Tamil Nadu, India
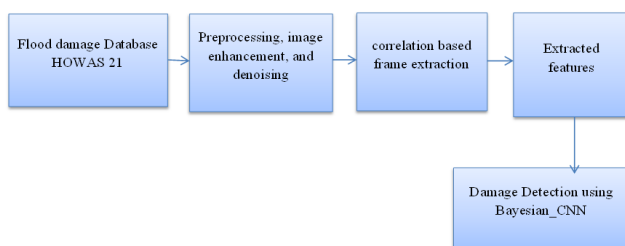[4]Department of Computer Science and Engineering, K Ramakrishnan College of Engineering, Tamil Nadu, India
*to whom all correspondence should be addressed: e-mail: muthuklakshmi56@gmail.com

Graphical abstract

Abstract

Flood management is the act of determining the frequency, magnitude, and duration of flood episodes based on the elements of a river basin that may be monitored. Floods endanger human lives and inflict significant property damage. It is essential for creating suitable flood risk management plans, lowering flood dangers, and evacuating people from flood-prone locations. Hydrodynamic methods for managing floods may be replaced with deep learning. Existing methods, however, concentrate on employing CNNs or RNNs to capture either the spatial or temporal flood patterns. Despite several advancements in flood control technology, less focus has been placed on minimising the damage that these systems do to the environment in order to boost their dependability and effectiveness. When the data is skewed, CNNs might overfit. We demonstrate how automated regularisation and uncertainty quantification allows Bayesian-CNN to get beyond these drawbacks. We have created a unique method to make use of the uncertainties that the Bayesian-CNN provides, which greatly improves performance on a big portion of the test data (around a 6% increase in accuracy on 77% of test data). By projecting the data into a low-dimensional space using a nonlinear dimensionality reduction approach, we also provide an entirely novel rationale for the uncertainty.

This dimensionality reduction makes it possible to visualize the test data for interpretation and displays the data's structure in a low-dimensional feature space. This paper discusses and makes use of uncertainties for flood control while demonstrating the benefits of Bayesian-CNN over state-of-the-art technology. As a consequence, the Bayesian-CNN obtains 95.7% F1-score, 99.3% F1-score, 98.5% precision, and 98.3% recall.

Keywords: Flood management, convolution neural network, environment damage, forecasting, deep learning

1. Introduction

Globally, the frequency of natural catastrophes has grown as a result of climate change. These natural occurrences, such as floods, droughts, fires, cyclones, hurricanes, and others, have significant effects on both developed and developing nations (Tsai *et al*., 2021). Recently, a lot of research has been done to create effective early warning systems and enhance disaster management techniques. Natural occurrences cannot be prevented, but efficient disaster management strategies may lessen the damage and the number of victims (Anbarasan *et al*., 2020). At each of the three phases of the event, many disaster management techniques are relevant (Gupta, 2020). The first phase, known as the pre-disaster stage, focuses on monitoring or an early warning system to inform the authorities of an impending natural catastrophe. The second phase, known as damage control during the event, and the third phase, known as post-disaster recovery, aim to restore normalcy (Shinta *et al*., 2020). The International Emergency Management System (IEMS) was formed in 1993 to build up processes and principles for nations to adjust during a crisis scenario to face the problems of natural occurrences. The most recent communication and information technology techniques may be utilized to improve the relief effort following a natural catastrophe, according to the Millenium Development Goals (MDG) 2015 (Kankanamge *et al*., 2020). With the use of new

technology, relief operations may be hastened to assist as many people as possible in a short amount of time. Therefore, constructing infrastructure that is robust to disasters and achieving good disaster management may benefit greatly from emerging technologies (Wu *et al.*, 2020). The area of catastrophe management procedure has a knowledge deficit. With the use of modern techniques, a special emphasis should be placed on climate change and the accompanying hazards. It is necessary to create advanced early warning systems based on the framework, algorithms, and ideas. The UN has set achieving catastrophe resilience as one of its main objectives to be accomplished by 2030 (Matgen *et al.*, 2007; Chen *et al.*, 2020). This goal has been highlighted by several nations across the globe. It may be reached through using human resources, creating cutting-edge technology, and boosting flexibility via government. Infrastructure and capacities for resilience should concentrate on minimizing disasters and financial losses (Elhag and Abdurahman, 2020). The only way ahead is to quickly identify the risk and use the right technologies to reduce it. The decision-making process is critical in all phases of crisis management because it affects the success of rescue missions and events (Shafizadeh-Moghadam *et al.*, 2018). Big data analysis is required for this decision-making, which is more difficult than regular data analysis. This emphasizes the need for computational intelligence, real-time algorithms, and data extraction and visualization techniques (Cao *et al.*, 2021). These algorithms must be able to make prompt judgments, examine various data formats, and extract the data. Computational intelligence is widely used in most flood management systems to make timely choices. The use of the computationally intelligent approach for flood control systems is gaining a lot of attention. The most recent computational techniques must be examined to pinpoint any gaps in flood control that still exist (Mohanty *et al.*, 2020). Applying artificial intelligence and machine learning algorithms for weather forecasts, flood-affected areas, damage identification, and other uses is a new trend in computational technology (Mishra and Arya, 2020). Researchers are also examining several methods for large-scale data analysis that would resolve real-time problems with the least amount of processing time.

- We suggest a new model to build on the Bayesian- CNN and call it the Modified Bayesian-CNN to further enhance its performance.
- The learnable parameter in the suggested adaptivity is random as opposed to the deterministic parameters described in the literature, which makes it innovative. As a result, the activation function is now selected from a set of similar functions using the probability distribution of parameters discovered via data analysis.

This paper is structured as follows: In section 2, related works for flood management and the detection of environmental degradation using neural networks are presented. In Section 3, the proposed feature extractor and classifier are described in detail. In section 4, the performance of the proposed model is presented alongside a comparison. In Section 5, the overarching inference for the proposed model is presented.

2. Related works

The findings of studies using deep neural networks for time-series data are excellent, and they provide a clear vision for expanding the use of neural network designs in time-series data. Researchers have shown the application of neural networks for forecasting financial time series, taxi demand, and traffic speed. Since both tasks depend on changes in linked nodes in the network, traffic speed prediction and flood management are highly comparable tasks.

Castangia *et al.* (2023) investigate the Transformer neural network (TNN)'s relevance to the task of flood forecasting. In comparison to recurrent networks, the Transformer has reduced computing expenses. The acquired forecasting errors are deemed acceptable by domain norms, confirming the Transformer's suitability for the job of flood forecasting. Chen *et al.* (2023) proposes a novel approach for the quick prediction of the danger of urban flooding by combining a numerical model with great computational efficiency with an LSTM artificial neural network model (LSTM+ANN) with high computational accuracy. The technique builds an LSTM neural network prediction model for each waterlogging location using simulation results from a numerical model of urban floods as the data driver. The focused time delay network (FTDN), layered recurrent Network (LRN), and nonlinear autoregressive network with exogenous inputs (NARX) networks are examples of dynamic networks. In (Wan *et al.*, 2023), a comprehensive framework was presented to consistently characterize these networks. Using a convolutional neural network (CNN), (Wang *et al.*, 2022) suggests a technique for forecasting the long-term temporal two-dimensional range and depth of flooding in all grid locations. The associated raster flood statistics were generated using a physical model, and the deep learning model was trained using a large rainfall dataset gathered from real flooding occurrences. A Deep Learning (DL) based flood management model is investigated and used for interpretation and prediction utilizing meteorological data in the (Chitra and Rajasekaran, 2022) proposed study to minimize computational and time complexity with high accuracy. The deep learning architecture used is called Gated Recurrent Networks (GRU), a variation of the recurrent neural network model that can efficiently employ historical data knowledge for prediction and is quicker in terms of training speed. In (Linh *et al.*, 2021), which examined the potential of a wavelet neural network (WNN) hybrid model to predict the maximum monthly discharge of a specific area, it was discovered that the WNN hybrid machine learning model consistently outperformed both the standalone artificial neural network (ANN) model and the multiple linear regression model in terms of performance in predicting flood discharges.

There are fewer papers accessible for the flood management process when older techniques of flood

management are examined. High complexity and comparatively poor prediction accuracy continue to plague statistical formula-based and numerical approaches. The asymmetry of the wind profile and the inability of the previous temporal-spatial wind speed model to accommodate many wind speed measurements were also issues that went unaddressed. As a result, a new deep neural network is built, as described below.

3. Proposed methodology

In this research, we developed a unique Bay_CNN method for detecting road damage in Flooding Management. The Bay_CNN method was developed to accurately categorize defective regions into their respective classes. The Bay_CNN method does this by using a preprocessor, a 3D-CNN-based feature extractor, and a Bayesian-CNN-based classification, as seen in Figure 1.
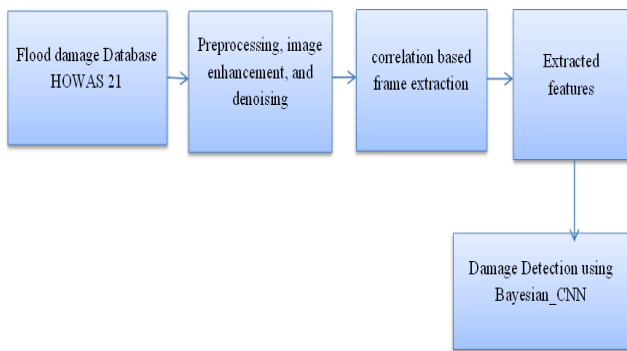

Figure 1. Block diagram for cyclone prediction

3.1. Dataset description

The Fluvial, Plumvial, and Groundwater Flood Damage Database HOWAS 21 includes object-specific flood damage data. The databases include different flood risk, exposure, susceptibility, and direct palpable damage characteristics for properties across several economic sectors. Six sectors are used by the database to classify object-specific damage:

- Private residences;
- The commercial and industrial sectors;
- Public municipal infrastructure (administration, social services, education, etc.);
- Agricultural structures;
- Wooded and agricultural land;
- Public thoroughfares, such as highways and other forms of transportation;
- Waterways and hydraulic features (especially those used for flood defense);
- Urban green areas.

HOWAS 21 includes a wide range of variables such as hazard characteristics (e.g., flow velocity, flood duration, and contamination), vulnerability parameters such as building characteristics (e.g., building shape, year of construction), precautionary measures, warning lead time, and flood consequences (e.g., absolute and relative damage to flood-affected objects, economic damage due to business interruption in the commercial sector).

3.2. Preprocessing of data

Preprocessing involves picture enhancement and denoising. The first method is carried out by computing the grey coefficient in the space domain and then correcting the coefficient of the image transformation before an inverse transformation is used to draw attention to the image flaws. The latter tries to suppress impulsive sounds, and salt-and-pepper noises, and to reduce picture blurring; while doing so, significant image structures should be retained. The fundamental unit of image accuracy and heterogeneity detection sensitivity is the grey level. The categorization is more favorable the higher the grey level resolution of the image and the richer the image information.

A single frame's Signal Noise Ratio (SNR)

$$SNR = \frac{xs}{\sigma n}.xn \qquad (1)$$

The image signal is denoted by xs, the noise by xn, and the variance of *xn* by σn. The frame's total SNR is

$$SNR = \frac{\sum_{i=1}^{m} xsi}{\sum_{i=1}^{m} xni} \qquad (2)$$

$$\sum_{i=1}^{m} xni.m\sigma n \qquad (3)$$

$$SNR = \frac{mxs}{m\sigma n} = Msnr \qquad (4)$$

Since then, the SNR has increased by m times. The key to image blurring is that the image is averaged or integrally processed such that it may be recovered by an inverse process. The second-order differential's edge placement capability is greater, and the sharpening impact is better than the first-order differential. The differential operation may emphasize picture features to make the image sharper. Define a discrete form of the second-order differential, then create a filter template based on this form to convolve with the image. This is the fundamental way to use the second-order differential operator. The rotation invariance of an isotropic filter means that its response is unaffected by the direction of an abrupt shift in the image. The features (mutations) that can be recognized at a specific place in the initial image may thus still be detected after the original image has been rotated by 90 degrees.

3.3. Feature extraction

Following preprocessing, the following characteristics of filtered damaged pictures are extracted. Some complex characteristics, including hot bags, gas tungsten components, and ray effects, have an impact on the extraction of damaged parts. Additionally, a data-driven model's output is significantly influenced by the dataset it is driven. As a result, the multi-dimensional feature extraction layer is recommended as the model's topmost layer. This layer may choose the variables that are best connected with the defect detection track from the attribute dimension. This layer may examine the most closely linked time window to the target timestamp from

the temporal dimension. This layer's goal is to minimize the size of the input variables and get rid of extraneous noise data, which may boost the efficiency and accuracy of predictions in the layers below. In this case, the ideal period is chosen using the Auto Correlation Function (ACF) and Partial Auto Correlation Function (PACF). In statistics, the Pearson Correlation (PC) between values of the process at various periods is the autocorrelation of a random process. Equation (5) is used to get the PCC for the first N -k values $L1$ ={$lt1$; $lt2$,….., $lt(N$-$k)$, and the final N - k values $L2$={ltk, $lt(k$C1),…., ltN}, respectively.

$$B1 = \frac{\sum_{i=1}^{N-K}\left(li - L1\right)\left(li + k - L2\right)}{\sqrt{\sum_{i=1}^{N-K}(li - L1)}\sqrt{\sum_{i=1}^{N-K}(li - L2)}} \tag{5}$$

where $L1$ and $L2$ are the averages of the most recent N-k values, respectively. The equation (60 for the autocorrelation coefficient at time lag k may be given by omitting the difference between $L1$ and $L2$

$$ACF = \frac{\sum_{i=1}^{N-K}\left(li - L1\right)\left(li + k - L1\right)}{\left(li - L1\right)^2} \tag{6}$$

The partial autocorrelation coefficient of time lag k, given the steel defects, tracks L= {$lt1$, $lt2$…..ltm}, relates to the effect of lt-k on lt after eliminating k - 1 random variables.

Equation (7) provides the PACF,

$$PACF = \frac{E\left[(lt - Elt)(lt - k - Elt - k)\right]}{E[lt - k - Elt - k)]} \tag{7}$$

The initial features F=$f1$, $f2$, fc will change to F'= {f1, f2….fd} where ($d \leq c$), once the multi-dimensional feature selection layer is applied, and the most correlated time range k is also chosen.

3.4. Classification using Bayesian-CNN

Short-term flood damage identification is still a difficult job to complete despite several advancements in artificial intelligence, machine learning, and statistical weather prediction models. As a result, Figure 2 illustrates the implementation of stochastic adaptive activation on Bayesian-CNN.
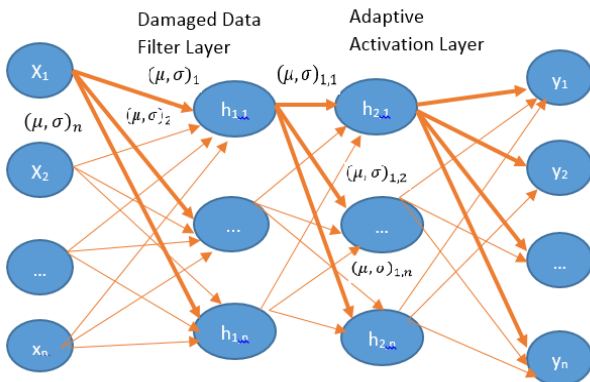
Figure 2. Architecture of Bayesian_CNN for the classification process

The parameters of CNNs are filters or kernels that must be learned during training. These kernels are represented by probability distributions in the case of a Bayesian CNN. These filters or kernels, which are of form h×w×d, are subjected to the reparameterization procedure while the Bayesian-CNN is being trained. They are generated using the following equation from the variational posterior $q(w|\theta)$:

$$w_{h,w,d} = \mu_{h,w,d} + log\left(1 + exp\left(\rho_{h,w,d}\right)\right)\varsigma_{h,w,d} \tag{8}$$

where the filter's height, breadth, and depth are h, w, and d, respectively, and stands for point-wise multiplication. Due to the probability distribution across the weights, Bayesian deep learning allows us to quantify the prediction's uncertainty. Using the predictive posterior probability distribution as an expectation: $E_{q(w|\theta)}[P(y'|x',w)$ gives us the most probable prediction of the unknown data x'. The predicted posterior probability distribution's variance: $Var_{q(w|\theta)}[P(y''|x'',w)]$quantifies the uncertainties. Aleatoric and epistemic uncertainties are the two different categories of uncertainty. The total of these two uncertainty is the variance of the predicted posterior probability distribution.

$$Var_{q(w|\theta)}[P\left(y''|x'',w\right) = aleatoric + epistemic \tag{9}$$

The variance of the predicted posterior probability distribution is used to calculate the uncertainties.

$$Var_{q(w|\theta)}[P\left(y''|x'',w\right) = E_{q(w|\theta)}[y - E[y]]^2 =$$
$$\int_{\delta_v}^{n}[[diag\left(E_{p(y'|x',w)}\left[y'\right]\right) - E_{p(y'|x',w)}\left[y'\right].k \tag{10}$$

The aforementioned term, which is derived from a specific application of the law of total variance, represents the sum of aleatoric and epistemic uncertainty. The equation of the aleatoric uncertainty is: $\frac{1}{N}\sum_{n=1}^{N}diag\left(p'_n\right) - p'_n p'^T_n$, where, p'n = p(w'n) = softmax{fw't(x')}. The formula for the epistemic uncertainty is as follows: $\frac{1}{N}\sum_{n=1}^{N}\left(p'_n - p'\right)\left(p'_n - p'\right)^T$, Where, p'n = p(w'n) = softmax{fw't(x')} and $p' = \sum_{n=1}^{N}\frac{p'_n}{n}.N$. The general formula for calculating variance is:

$$Var_{q(w|\theta)}[P\left((y'|x',w\right)] = [\frac{1}{N}\sum_{n=1}^{N}diag\left(p'_n\right) - p'_n p'^T_n]$$
$$+ [\frac{1}{N}\sum_{n=1}^{N}(p'_n - p')(p'_n - p')^T] \tag{11}$$

Eq. 11 may be used to determine the variance of the predictive distribution, which tells us how confident the network is in its ability to forecast an image. Exploding or disappearing gradients are possibilities when attempting to quantify uncertainty. As a result, a perceptron's learning capabilities and training complexity trade-off in a way that may be optimized. This is accomplished by modifying the Bayesian CNN and adding a stochastic activation function that can be learned and adjusted to the training set. A probabilistic parameter that is learned

during the neural network's training is a part of this adaptive activation function. To do this, the activation functions of a Bayesian-CNN are changed by the addition of a trainable probabilistic hyperparameter ($\propto$) meter (α). Below are the specifics of the suggested adaptive activation function:

$$\sigma\left(\alpha f_k\left(x^{k-1}\right)\right) \tag{12}$$

Where,

$$f_k\left(x^{k-1}\right) = w'^k x^{k-1} + b^k \tag{13}$$

σ is the activation function, α is the trainable probabilistic hyperparameter, w' and b are the weight and bias of the kth layer and x^{k-1} is the results of the neural network's previous layer. The loss function F is changed to include the extra stochastic parameter $\propto$ to integrate the stochastic adaptive activation. more particularly, the collection of trainable network characteristics w = {w',b} in F is extended to w = {w',b,$\propto$}. So, the modified loss function F'(D,θ) is

$$F'\left(D,\theta\right) = \sum_{i=1}^{n}[\log q\left(\left(W^{(i)}|\theta\right) - log P\left(W^{(i)}\right) - log P\left(D|W^{(i)}\right)\right) \tag{14}$$

As with the parameters w, the parameter α is also learned. The posterior distribution for the parameter α is determined using Bayes' rule under the assumption that the parameter has a prior distribution (a mixture of Gaussian). A Gaussian variational posterior $q_\propto$ with a mean of $\mu_\propto$ and a standard deviation of $\sigma_\propto$ comes the closest to representing this posterior distribution. Gradient descent is used to update this variational posterior's parameters as,

$$\mu_\alpha^{m+1} = \mu_\alpha^m - \gamma \nabla_{\mu\alpha} F^m \tag{15}$$

and

$$\sigma_\alpha^{m+1} = \sigma_\alpha^m - \gamma \nabla_\alpha F^m \tag{16}$$

where the pace of learning is γ. For the fully connected layers in this study, an adaptive ReLu provided by $\sigma(\delta)$ max $(0, \delta x)$ is used.

4. Performance analysis

Tables 1 and 2 lists the total number of damage reports per economic sector included in HOWAS 21 as well as the average data availability rate for non-mandatory variables under the minimal standards for data inclusion into HOWAS 21.

Table 1. Dataset description

Sector	Total number of images	Fraction of the total number	Average data
Private households	4882	57.1	42
Commercial and Industrial	2905	33.9	21.8
Public thoroughfare, road, and transport infrastructure	246	2.9	51.7
Watercourses and hydraulic structure	525	6.1	43.5
Agricultural and forested land	137	-	-
Urban open spaces	237	-	-
Total	**8932**	**100**	**100**

Figure 3(a). Comparison of the Bayesian-CNN system for Training

Figure 3(b). Comparison of the Bayesian-CNN system for Testing

Figure 4(a). Comparison of Bayesian-CNN system for Training

Figure 4(b). Comparison of the Bayesian-CNN system for Testing

In Figures 3(a) and 3(b) simulation was run with a split of the data into 80:20, and different numbers of images from 100, 200, 300, 400, and 500 were utilized as inputs. Next, the comparison is evaluated as seen in Figure 3. As a consequence, during 80% of the training, the established

Bayesian-CNN obtains 99.4% accuracy, 97.4% precision, 94.6% recall, and 95.3% F1-score. Additionally, for 20% of testing, it scores 98.4% accuracy, 97.3% precision, 94.3% recall, and 95.3% F1-score (Tables 3 and 4).

**Table 2.** Damage classifier outcome of Bayesian-CNN system for 80:20

Number of images	$Accu_{racy}$	$Prec_n$	$Reca_u$	F_{score}
Training (80%)				
100	98	96	93	95.5
200	99	97	95	94.8
300	99.5	98	94	96.2
400	99.7	97.5	95.5	95.1
500	99.2	97.9	94.2	94.9
Average	**99.4**	**97.4**	**94.6**	**95.3**
Testing (20%)				
100	98.6	96.5	93.5	94.8
200	97.9	97.8	94.8	95.7
300	99.2	97.2	95.2	95.5
400	98.8	97.6	93.1	95.2
500	97.5	98.1	94.6	95.1
Average	**98.4**	**97.3**	**94.3**	**95.3**

Table 3. Damage classifier outcome of Bayesian-CNN system for 70:30

Number of images	$Accu_{racy}$	$Prec_n$	$Reca_u$	Fscore
Training (70%)				
100	98.2	96.8	95.8	97.2
200	97.8	97.2	97.2	96.5
300	99.1	97.5	96.5	96.9
400	98.9	97.9	96.9	96.3
500	98.6	97.7	96.1	97.1
Average	**98.4**	**97.3**	**96.4**	**96.8**
Testing (30%)				
100	98.2	97.8	93.5	94.8
200	98.8	97.2	94.8	95.7
300	99.0	97.5	95.2	95.5
400	97.9	96.9	93.1	95.2
500	98.7	97.1	94.6	95.1
Average	**98.6**	**97.3**	**94.3**	**95.3**

Table 4. Comparative analysis between existing and proposed methods

Methods	$Accu_{racy}$	$Prec_n$	$Reca_u$	Fscore
TNN [14]	91	90	93	92
LSTM+ANN [15]	92	89	91	90
GRU [18]	90	87	85	83
WNN [19]	89	88	86	82
Bayesian-CNN [proposed]	99.3	98.5	96.4	95.7
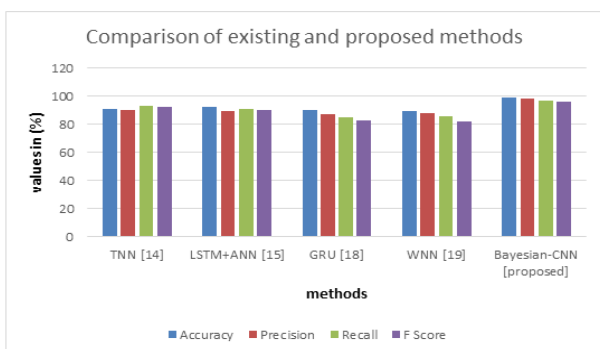
Figure 5. Comparison between existing and proposed methods

The data is divided into two halves of 70:30, and simulations were run with varying numbers of input images from 100, 200, 300, 400, and 500 as shown in Figures 4(a) and 4(b). Next, the comparison is evaluated as seen in Figure 4. As a consequence, during 70% of the training, the established Bayesian-CNN obtains 98.4% accuracy, 97.3% precision, 96.4% recall, and 96.8% F1-score. Additionally, for 20% of testing, it scores 98.6% accuracy, 97.3% precision, 94.3% recall, and 95.3% F1-score.

Figure 5 defines the overall comparative analysis between existing and proposed methods. The proposed Bayesian-

CNN method demonstrates exceptional performance, achieving the highest accuracy (99.3%) among all the methods. It also showcases impressive precision (98.5%), recall (96.4%), and F-score (95.7%) values. These results highlight the effectiveness of the Bayesian-CNN approach in accurately classifying the task at hand. The high accuracy indicates that a significant proportion of the predictions made by the model are correct, while the high precision and recall values suggest a good balance between identifying true positive instances and minimizing false negatives. The impressive F-score reflects the harmonic mean of precision and recall, capturing the overall effectiveness of the model. Overall, the proposed Bayesian-CNN method showcases superior performance and holds promise for the given task compared to the other evaluated methods.

5. Conclusion

We were able to demonstrate the effectiveness of Bayesian-CNN for damage classification by utilizing the framework we developed for assessing environmental damage. Our classification model demonstrated a high degree of adaptability that may be employed throughout a spectrum of hurricane and other coastal hazard occurrences, given the relatively few and wide range of images used for the input data set.

5.1. Findings and implications

The findings of the proposed model demonstrate the model's capacity to quickly and accurately identify damaged sections of buildings and structures from test data, which is essential for more accurate damage assessment. It yields benefits including reduced risk of harm to society, human health, economic activities, infrastructure, cultural heritage, and the environment.

5.2. Limitation of proposed method

A good physical understanding of the hydrologic process can aid in the selection of the input vector and the design of a more efficient network which will leads to better results. But our proposed method is not concentrated on hydrologic process.

5.3. Future enhancement

Further studies exploring the use of transfer learning approaches to develop classification and object identification models trained on post-disaster images may enhance our work. The amount of time needed for damage assessment would be greatly decreased by using these machine-learning models. Therefore, the hours to days needed to calculate the entire damage sustained may be avoided if relief plans were developed in the aftermath of a future coastal catastrophe. As a consequence of the direct deployment of artificial intelligence technologies such as our categorization and object identification algorithms, damaged coastal communities would be able to obtain more accurate and timely help.

References

Tsai M.H., Yang C.H., Chen J.Y. and Kang S.C. (2021). Four-stage framework for implementing a chatbot system in disaster emergency operation data management: A flood disaster management case study. *KSCE Journal of Civil Engineering*, **25**, 503–515.

Anbarasan M., Muthu B., Sivaparthipan C.B., Sundarasekar R., Kadry S., Krishnamoorthy S. and Dasel A.A. (2020). Detection of flood disaster system based on IoT, big data and convolutional deep neural network. *Computer Communications*, **150**, 150–157.

Gupta K. (2020). Challenges in developing urban flood resilience in India. *Philosophical Transactions of the Royal Society A*, **378**(2168), 20190211.

Oktani Maya Shinta E., Suryadi B. and Riduansyah Syafari M. (2020). Performance Assessment of Local Government Organizations on Flood Disaster Prevention and Preparedness in Gunung Mas Regency.

Kankanamge N., Yigitcanlar T., Goonetilleke A. and Kamruzzaman M. (2020). Determining disaster severity through social media analysis: Testing the methodology with South East Queensland Flood tweets. *International Journal of Disaster Risk Reduction*, **42**, 101360.

Wu Z., Shen Y., Wang H., and Wu M. (2020). Urban flood disaster risk evaluation based on ontology and Bayesian Network. *Journal of Hydrology*, **583**, 124596.

Matgen P., Schumann G., Henry J.B., Hoffmann L. and Pfister L. (2007). Integration of SAR-derived river inundation areas, high-precision topographic data and a river flow model toward near real-time flood management. *International Journal of Applied Earth Observation and Geoinformation*, **9**(3), 247-263.

Chen J., Li Q., Wang H. and Deng M. (2020). A machine learning ensemble approach based on random forest and radial basis function neural network for risk evaluation of regional flood disaster: a case study of the Yangtze River Delta, China. *International Journal of Environmental Research and Public Health*, **17**(1), 49.

Elhag M. and Abdurahman S.G. (2020). Advanced remote sensing techniques in flash flood delineation in Tabuk City, Saudi Arabia. *Natural Hazards*, **103**(3), 3401–3413.

Shafizadeh-Moghadam H., Valavi R., Shahabi H., Chapi K. and Shirzadi A. (2018). Novel forecasting approaches using combination of machine learning and statistical models for flood susceptibility mapping. *Journal of Environmental Management*, **217**, 1–11.

Cao C., Xu M., Kamsing P., Boonprong S., Yomwan P. and Saokarn A. (2021). *Environmental Remote Sensing in Flooding Areas*. Springer, Singapore. https://doi.org/10.1007/978-981-15-8202-8.

Mohanty M.P., Nithya S., Nair A.S., Indu J., Ghosh S., Bhatt C.M. and Karmakar S. (2020). Sensitivity of various topographic data in flood management: Implications on inundation mapping over large data-scarce regions. *Journal of Hydrology*, **590**, 125523.

Mishra A. and Arya D.S. (2020). Development of decision support system (DSS) for urban flood management: a review of methodologies and results. In *World Environmental and Water Resources Congress,* Reston, VA: American Society of Civil Engineers, pp. 60–72.

Castangia M., Grajales L.M.M., Aliberti A., Rossi C., Macii A., Macii E. and Patti E. (2023). Transformer neural networks for interpretable flood forecasting, *Environmental Modelling & Software*, **160**, 105581

Chen J., Li Y., Zhang C., Tian Y., and Guo Z. (2023). Urban flooding prediction method based on the combination of LSTM neural network and numerical model. *International Journal of Environmental Research and Public Health*, **20**(2), 1043.

Wan X., Wu Q., Cao Z. and Wu Y. (2023). Real-time flood forecasting based on a general dynamic neural network framework. *Stochastic Environmental Research and Risk Assessment*, **37**(1), 133–151.

Wang H.W., Lin G.F., Hsu C.T., Wu S.J. and Tfwala S.S. (2022). Long-term temporal flood predictions made using convolutional neural networks. *Water*, **14**(24), 4134.

Chitra P. and Rajasekaran U.M. (2022). Time-series analysis and flood prediction using a deep learning approach. In, *2022; International Conference on Wireless Communications Signal Processing and Networking (WiSPNET)* (139–142). IEEE.

Linh N.T.T., Ruigar H., Golian S., Bawoke G.T., Gupta V., Rahman K.U. and Pham Q.B. (2021). Flood prediction based on climatic signals using wavelet neural network. *Acta Geophysica*, **69**(4), 1413–1426.